High Gain Submicrometer Optical Amplifier at Near-Infrared Communication Band

Xiaoxia Wang,[1] Xiujuan Zhuang,[1] Sen Yang,[2] Yu Chen,[2] Qinglin Zhang,[1] Xiaoli Zhu,[1] Hong Zhou,[1] Pengfei Guo,[1] Junwu Liang,[1] Yu Huang,[2] Anlian Pan,[1,*] and Xiangfeng Duan[3,†]

[1]*Key Laboratory for MicroNano Physics and Technology of Hunan Province, School of Physics and Electronic Science, and State Key Laboratory of Chemo/Biosensing and Chemometrics, Hunan University Changsha, Hunan 410082, People's Republic of China*

[2]*Department of Materials Science and Engineering, University of California, Los Angeles, California 90095, USA*

[3]*Department of Chemistry and Biochemistry, University of California, Los Angeles, California 90095, USA*

(Received 29 April 2015; published 10 July 2015)

Nanoscale near-infrared optical amplification is important but remains a challenge to achieve. Here we report a unique design of silicon and erbium silicate core-shell nanowires for high gain submicrometer optical amplification in the near-infrared communication band. The high refraction index silicon core is used to tightly confine the optical field within the submicron structures, and the single crystalline erbium-ytterbium silicates shell is used as the highly efficient gain medium. Both theoretical and experimental results show that, by systematically tuning the core diameter and shell thickness, a large portion of the optical power can be selectively confined to the erbium silicate shell gain medium to enable a low loss waveguide and high gain optical amplifier. Experimental results further demonstrate that an optimized core-shell nanowire can exhibit an excellent net gain up to 31 dB mm^{-1}, which is more than 20 times larger than the previously reported best results on the micron-scale optical amplifiers.

DOI: 10.1103/PhysRevLett.115.027403 PACS numbers: 78.67.Uh, 42.70.-a, 81.07.Gf

Waveguides and amplifiers represent the central components for optical communication and amplification. The erbium-doped fiber or waveguide amplifiers (EDFA or EDWA) represent the standard commercial amplifiers in current optical communication systems [1–9]. In such systems, the erbium ions are used as the optically active elements because their intra-4f transition matches well with the standard communication band at 1.54 μm. Most optical amplifiers working at communication bands today require a size on the micrometer level or larger [2–4,6,8,9]. With the continued progress in information technology, the miniaturization of such fiber or waveguide amplifiers is of considerable interest for developing on-chip photonic integration and chip-scale optical communication [10–16]. However, there is limited progress on submicrometer scale amplifiers to date. Although metal or gain medium hybrid nanostructures have been reported recently to achieve light amplification via a surface plasmon polariton at the visible region [17–19], submicrometer optical amplifiers in the infrared communication band remain a significant challenge; this is because of the exceptionally large propagation loss from the weak optical confinement in the infrared wave band [2,3,7], and the low medium gain due to the very limited concentration of the erbium ions doped in the materials.

Erbium silicates have recently received considerable attention as a potential high gain medium for optical amplification in the communication band, due to their high-quality single crystalline nature and high density of optically active Er^{3+} ($\sim 10^{22}$ cm^{-3}) [20–24], compared to that of the conventional erbium doped silicon or silicate materials (10^{19} cm^{-3}) [25]. In order to increase the absorption cross section in the near-infrared region, ytterbium ions (Yb^{3+}) are usually codoped as a sensitizer [26]. Ytterbium-ion-codoped erbium silicate is therefore expected to be an attractive high-gain medium material for optical amplification at the near-infrared communication band. However, the efforts in improving the material properties are not enough to overcome the bottleneck in achieving integrated submicrometer optical amplifiers. A novel structure design used to enhance the optical confinement must be considered.

With a high refractive index (3.5 at a wavelength of 1550 nm), silicon nanowires have recently been explored as low-loss submicrometer waveguides that can offer the possibility of reducing the footprint of optical components for on-chip photonic integration [27–30]. Here we report a unique design of silicon-erbium-ytterbium silicate (Si-EYS) core-shell nanowires as high gain submicrometer optical amplifiers in the near-infrared communication band. In this nanowire, the high refraction index silicon core is used to tightly confine the optical field within the submicron core-shell nanowires, and the erbium silicate shell is used as the highly efficient gain medium [Fig. 1(a)]. The theoretical model to demonstrate the basic physical concept about electromagnetic field mode distribution in a nanostructure can be described using the Helmholtz equation [31],

$$\frac{1}{r}\frac{\partial}{\partial r}\left(r\frac{\partial \boldsymbol{\Psi}}{\partial r}\right)+\frac{1}{r^2}\frac{\partial^2 \boldsymbol{\Psi}}{\partial \varphi^2}+k_0^2\left(n_i^2-n_{\mathrm{eff}}^2\right)\Psi=0, \quad (1)$$

where $\Psi = H_z$ and E_z are the z components of the magnetic and electric fields of the optical field. $k_0 = \omega/c$ is the free space wave number; ω is the angular frequency; c is the speed of light in vacuum; n_i represents the refractive index of the silicon core (n_1), erbium silicate shell (n_2), and vacuum (n_3), and n_{eff} is the effective index to be obtained and usually satisfies the relation $n_2 \leq n_{\text{eff}} \leq n_1$. For a given total nanowire diameter and the wavelength of propagation light, the optical confinement ability is mainly determined by the value of n_{eff} of guided modes that are supported in the nanowire [32].

Considering the continuity of the electromagnetic field at the boundary, we calculated the effective index by the finite element method for a 600-nm-diameter nanowire with different silicon core sizes [Fig. 1(b)]. It is found that the n_{eff} values for all modes supported in the core-shell nanowires increase from $n = 1.0$ (air index) to $n = 3.5$ (silicon index) when the core diameter varies from 0 to 600 nm. Near the cutoff area for each mode, the effective indexes are close to the value of air, which indicates weak mode confinement. The electrical field intensity distribution images of all the four existing modes were also simulated for the core-shell structures [see Fig. S1 in the Supplemental Material [33]]. Figure 1(c) shows the percentage of optical power confined within the nanowire for all the supported modes as a function of silicon core diameter, which indicates that the overall optical confinement can be greatly improved with increasing the silicon core size. For example, for the HE_{11} mode, only 32% power is contained in the wire for a pure EYS nanowire without silicon core, while more than 95% of optical power is confined in the nanowire when the silicon core diameter is increased above 300 nm. It is noted that the TE01 mode and HE21 mode are only supported when the core diameter is larger than 340 nm and 520 nm, respectively. At a core diameter of ~300 nm, the TM01 mode may be supported but typically with much lower coupling efficiency and guide optical power is mostly distributed outside of nanowire. Therefore, HE11 mode is the dominant one in our nanowire waveguide (see Fig. S2 in the Supplemental Material [33]). Since the silicate shell is the gain medium area, the confinement of the optical field within the shell is crucial for achieving an optical gain. Importantly, by carefully tuning the core diameter and shell thickness, a large portion of the optical power can be selectively confined to the erbium silicate shell gain medium to enable a low loss waveguide and high gain optical amplifier. The calculated results clearly show that the power confined in the silicate shell region for the main HE11 and TM01 modes have maximal values at the core diameter around 260 nm and 300 nm, respectively [Fig. 1(d)].

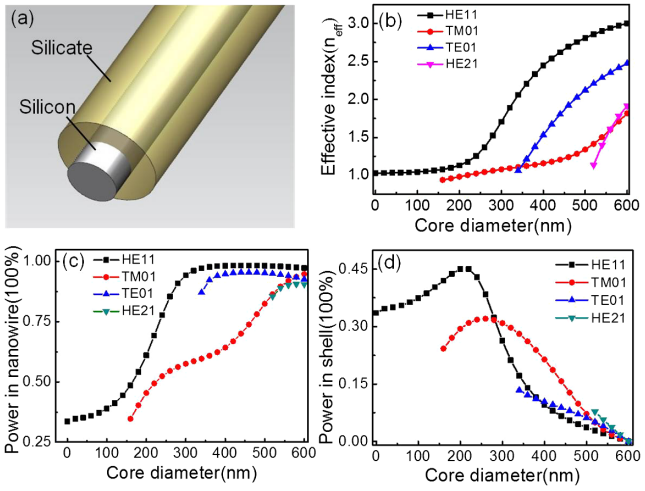

FIG. 1 (color online). (a) Schematic of the core-shell nanostructure. (b) The silicon core diameter-dependent effective index for guided modes that are supported in the core-shell Si-EYS nanowires at the wavelength of 1550 nm. (c) Simulated power percentage confined in the core-shell Si-EYS nanowire. (d) Simulated power percentage contained in the shell region.

Figures 2(a)–2(f) give the representative electrical field intensity distribution of the HE11 mode for a 600-nm-diameter nanowire with different silicon core sizes, which further intuitively demonstrates that the optical power confined in the nanowires increases with increasing the core diameter. It is evident that a large portion of the optical power can be well confined in the silicate shell when the core diameter is about 200–300 nm [Figs. 2(c) and 2(d)], which is essential for achieving high gain optical amplifier. Together, these analyses clearly demonstrate that the Si-EYS core-shell nanowires have excellent ability that can confine the infrared light at 1550 nm in a high gain medium at the submicrometer scale.

The Si-EYS core-shell nanowires can be grown using an Au-catalyzed chemical vapor deposition (CVD) route (see details in the Supplemental Material [33]). The typical scanning electron microscope (SEM) images [Figs. 3(a) and 3(b)] indicate that the resulting nanowires have a uniform diameter and a highly smooth surface. The cross-sectional transmission electron microscope (TEM) image

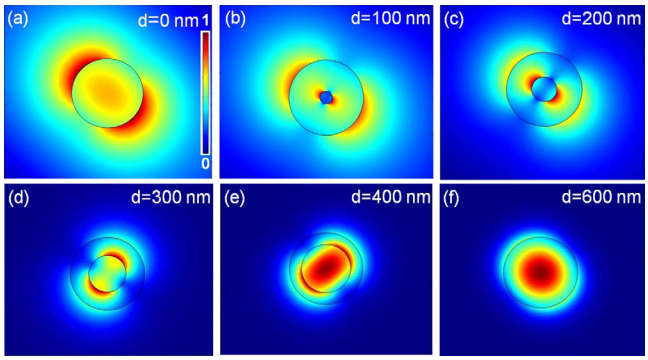

FIG. 2 (color online). (a)–(f) Optical electrical-field distribution images for HE11 mode with core diameters of 0 nm, 100 nm, 200 nm, 300 nm, 400 nm, and 600 nm (total diameter, 600 nm).

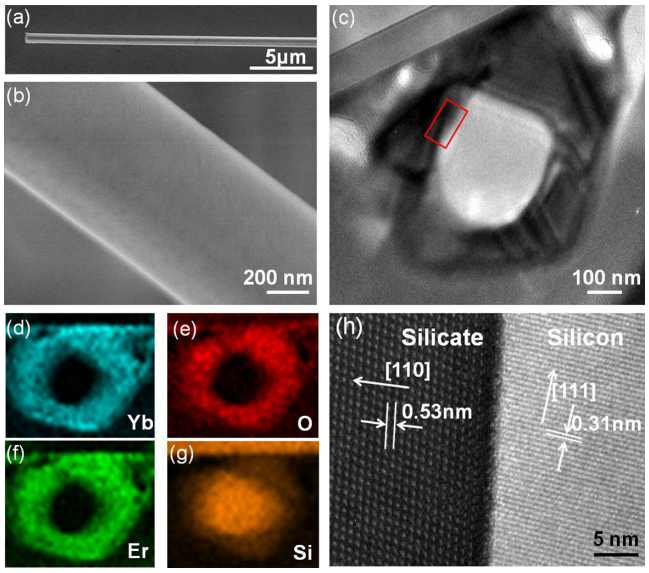

FIG. 3 (color online). Microstructure characterization of the Si-EYS core-shell nanowires. (a) Typical SEM images of part of a single nanowire, and (b) its locally amplified image. (c) Cross-sectional TEM image of the wire, and its corresponding two-dimensional element mapping (d)–(g). (h) Typical HRTEM image collected at the core-shell interface of the wire [red rectangle area in (c)].

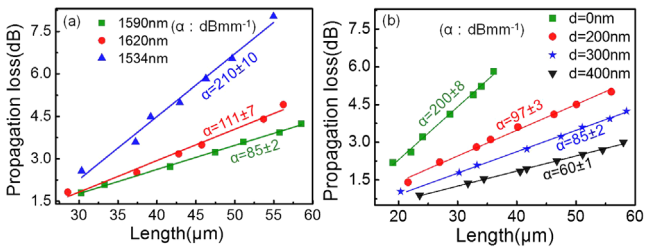

FIG. 4 (color online). (a) Guided length-dependent propagation loss at wavelengths of 1590 nm, 1620 nm, and 1534 nm, along a core-shell nanowire with a diameter of 600 nm (core diameter, 300 nm) and a length of 60 μm. (b) Guided length-dependent propagation loss at wavelength 1590 nm along four different nanowires with diameter of 600 nm and core diameters of 0 nm, 200 nm, 300 nm, and 400 nm. The solid lines in (a) and (b) are the linear fit of these measured data.

[Fig. 3(c)] of a representative wire and the corresponding 2D elemental mappings [Figs. 3(d)–3(g)] show clear core-shell structure, with the high refractive index silicon (Si) as the core and the high gain material, erbium ytterbium silicate (EYS) as the shell [Fig. 1(a)]. High-resolution TEM (HRTEM) studies show both the core and the shell are highly crystallized [Fig. 3(h)].

The propagation loss of the Si-EYS core-shell nanowires in the 1.5 μm band was systematically examined (see the Supplemental Material [33]). Figure 4(a) shows the guided length-dependent propagation loss for a 600-nm-diameter nanowire with the core diameter of 300 nm measured at the wavelengths of 1590 nm, 1620 nm, and 1534 nm, respectively. Based on these results, the loss coefficients α can be fitted [Fig. S5(c) in the Supplemental Material [33]]. We noted that the loss coefficient $\alpha = 210 \pm 10$ dB mm^{-1} at 1534 nm is considerably larger than those at 1590 nm ($\alpha = 85 \pm 2$ dB mm^{-1}) and 1620 nm ($\alpha = 111 \pm 7$ dB mm^{-1}), due to the existent intrinsic material absorption band of Er^{3+} at 1534 nm. The loss coefficients at 1620 nm and 1590 nm are mainly attributed to the structure-related propagation losses in the absence of the intrinsic material absorption. The loss coefficient of 111 ± 7 dB mm^{-1} at 1620 nm is slightly larger than that of 85 ± 2 dB mm^{-1} at 1590 nm, because of the weaker optical confinement effect at the longer wavelength.

The simulation results shown above (see Fig. 1) indicate that, in addition to the overall diameter, the structure-related propagation losses are also highly dependent on the size of the silicon core. Figure 4(b) shows the propagation loss at 1590 nm for the 600-nm-diameter nanowire with the core diameters of 0 nm (pure EYS nanowire), 200 nm, 300 nm, and 400 nm, respectively. It is apparent that the propagation loss decreases with increasing silicon core size. A propagation loss of 60 ± 1 dB mm^{-1} was achieved for the 400 nm core diameter nanowire (black triangle), which is only one third of that of pure EYS nanowires with the same overall diameter (200 ± 8 dB mm^{-1}, zero core diameters, green quadrangle symbols). The measured propagation loss is considerably larger than those of the conventional large dimension EDWA [4]. The relatively high loss may be partly attributed to the two-photon absorption process in the erbium silicate shell due to a highly confined optical field [42]. Additionally, the optical scattering loss resulting from slight structure irregularities, defects, and refractive index inhomogeneity is also non-negligible in such an ultrasmall waveguide.

To realize the light amplification based on these Si-EYS core-shell nanowires, a semiconductor laser at 980 nm is used as a pumping source. The dark-field optical image of the pumped nanowire shows clear photoluminescence (PL) emission from the surface of the entire nanowire. When a probe laser and the pump laser (980 nm) were simultaneously launched into the wire, the observed light emission from the surface was greatly decreased, indicating the transition from the random spontaneous emission into the coherent stimulated emission induced by the probe light (Fig. S6 in the Supplemental Material [33]). The optical amplification can be quantitatively demonstrated from the spectral measurements [Fig. 5(a)]. When only the pump laser is coupled into the nanowire waveguide, a relatively weak and broad spectrum is seen at the output end, consistent with the expected PL spectral feature of EYS. When only the probe laser at 1534 nm is coupled into the nanowire waveguide, a sharp peak of the same wavelength is seen at the output end consistent with the expected waveguiding effect. When both the pump and the probe

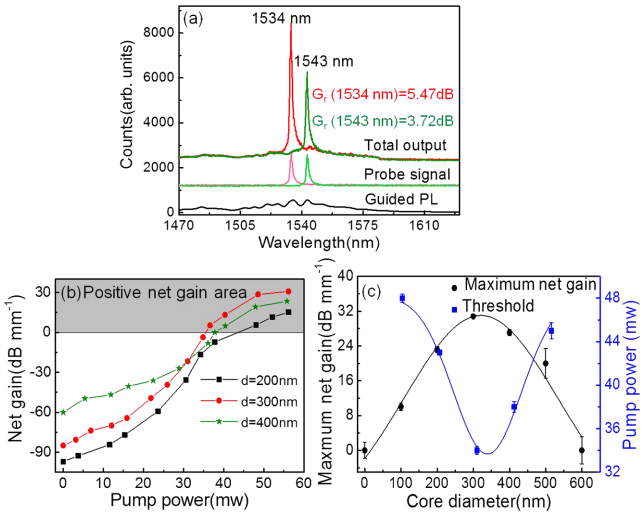

FIG. 5 (color online). (a) Typical spectra of the guided PL (black) only with the pump laser on; the probe laser at 1534 nm or 1543 nm, and the total output with both the probe and the pump lasers are present (pumped at 36 mW). (b) Pump power-dependent net gain for the wires with core diameters of d = 200 nm, 300 nm, and 400 nm (wire diameter is 600 nm). (c) Silicon core diameter-dependent maximum net gain (black dot, pumped at 56 mW) and positive net gain threshold (blue rectangular) for different silicon core diameters.

lasers are coupled into the nanowire, a much stronger signal at 1534 nm is observed at the output end. Significantly, it is noted that the peak intensity at 1534 nm is about 5 times stronger than that without the pump light, clearly demonstrating that there is an optical amplification effect taking place. A similar amplification effect was also observed at other wavelengths [e.g., 1543 nm in Fig. 5(a)], but with smaller amplification factors. These different amplification factors show a high degree of consistency with the PL spectral feature of EYS (see Fig. S7 in [33]). It is important to note that the frequency and the full width at half maximum (FWHM) of the total output light spectrum are identical with those of the output probe signal light, further demonstrating that the amplified light results from the stimulated amplification instead of the amplified spontaneous emission (ASE).

Both relative gain (G_r) and unit net gain (G_n) were used to quantify the optical amplification in these nanowires [33]. Considering the intensity of the amplified optical spectrum at 1534 nm is ~4 times larger than that of the output probe light intensity [Fig. 5(a)], we can obtain a relative gain (G_r) of 5.47 dB or 91 dB mm^{-1} for the wire. After comparing with the propagation loss of 85 dB mm^{-1}, we note that this relative gain can completely compensate the propagation loss to obtain a net gain (G_n) of 6 dB mm^{-1}.

We have further investigated the pump-power-dependent unit net gain in three 600 nm diameter nanowires with different core diameter of 200 nm (black quadrangle), 300 nm (red circle), and 400 nm (blue star) [Fig. 5(b)]. The net gains are negative at low pumping power for all three wires, indicating that the propagation losses cannot be compensated by the optical gain under weak pumping intensity. The net gain increases with increasing pumping power, and can eventually reach the positive net gain region [gray region in Fig. 5(b)] when the pumping power exceeds a certain threshold.

Figure 5(c) further plots the maximal net gain (black dot) achieved in the 600-nm-diameter nanowire waveguide as well as the positive net gain pumping threshold (blue rectangular) as a function of the silicon core diameter. The plot shows several important features. First, it is apparent that the maximal net gain first increases and then decreases with the core diameter varying from zero to 600 nm, with a peak value ($\sim 31 \pm 2$ dB mm^{-1}) obtained at the core diameter of around 300 nm. No positive net gain can be achieved in pure EYS wires with zero core diameters, because the propagation loss of ~200 dB mm^{-1} [see Fig. 4(b)] is too large to be completely compensated by the gain. Without the gain medium, the wires with 600-nm core diameter (pure silicon) also have no positive net gain, in spite of the low propagation loss. Second, the pumping threshold to reach the positive net gain value first decreases and then increases with the core diameter changing from 100 nm to 500 nm, and the nanowire with 300 nm core diameter exhibits a lowest positive gain pumping threshold. It is interesting to note that although the propagation loss of the nanowire with 300 nm core diameter is larger than that of the nanowire with 400 nm core diameter [see Fig. 4(b)], the positive net gain pumping threshold of the former is lower than that of the latter, which can be attributed to the increased gain medium in the nanowires with a smaller core size. More importantly, it is clearly found from Fig. 5(c) that the lower the net gain pumping threshold, the higher the maximal net gain value achieved, for the silicon core diameter ranging from 100 nm to 500 nm. The optimized core size for the best amplification performance is at around 300 nm, which has the lowest net gain pumping threshold and the highest maximal net gain, which is well consistent with the simulated results shown in Fig. 1(d).

The maximal net gain of $\sim 31 \pm 2$ dB mm^{-1} obtained in our Si-EYS core-shell nanowire waveguide amplifier is 23 times higher than the previously reported best gain value of 1.36 dB mm^{-1} for a microscale erbium-ytterbium codoped phosphate glass optical waveguide amplifier [4] (width, 4 μm; height, 1 μm) at the communication band (Table S1 in the Supplemental Material [33]). The unique design of the core-shell nanowire structure is essential for the realization of such excellent submicrometer amplifiers, which not only provides an excellent confinement of the guided infrared light by using the high refractive index silicon core, but also effectively integrates the high gain material in the silicate shell with a high density of Er^{3+} ions (4.8×10^{21} cm^{-3}).

In summary, we have reported a unique design of silicon and erbium silicate core-shell nanowires as high gain submicrometer optical amplifiers in the near-infrared communication band, in which the high refraction index silicon core is used to tightly confine the optical field within the submicron core-shell nanowires, and the erbium silicates shell is used as the highly efficient gain medium. By systematically tuning the core diameter and shell thickness, we show a large portion of the optical power can be selectively confined to the erbium silicate shell gain medium to enable a low loss waveguide and high gain optical amplifier. Significantly, we demonstrate that a 600-nm core-shell nanowire with 300-nm core can exhibit an excellent net gain up to 31 dB mm^{-1}, which is, to the best of our knowledge, more than 20 times larger than previously reported results on the micron-scale optical amplifiers [4]. Such a nanowire-based optical amplifier may be integrated into on-chip photonic circuits by using the well-developed guided-growth [43] or directed-assembly [44] approaches. Additionally, our design may also be realized using lithographically defined silicon nanowires with a coated erbium silicate shell, which can be readily integrated into current silicon photonic technology. These high gain nanoscale optical amplifiers could play an important role in high-density on-chip optical integration for faster processing speeds, larger information capacity, and lower power consumption. Together, our study opens a new pathway toward a submicrometer optical amplifier with high gain in the infrared communication band, marking an important step toward efficient on-chip photonic integration.

The authors are grateful to the National Natural Science Foundation of China (No. 11374092, No. 61474040, No. 11204073), the National Basic Research Program of China (No. 2012CB933703), the Aid Program for Science and Technology Innovative Research Team in Higher Educational Institutions of Hunan Province, the Hunan Provincial Science and Technology Department (No. 2014FJ2001, No. 2014GK3015, No. 2014TT1004). All authors thank Prof. Wei Zhang for valuable discussions.

X. W. and X. Z contributed equally to this work.

*Corresponding author.
anlian.pan@hnu.edu.cn
†Corresponding author.
xduan@chem.ucla.edu

[1] H. Q. Ye, Z. Li, Y. Peng, C. C. Wang, T. Y. Li, Y. X. Zheng, A. Sapelkin, G. Adamopoulos, I. Hernández, P. B. Wyatt, and W. P. Gillin, Nat. Mater. **13**, 382 (2014).
[2] L. H. Slooff, A. van Blaaderen, A. Polman, G. A. Hebbink, S. I. Klink, F. C. J. M. Van Veggel, D. N. Reinhoudt, and J. W. Hofstraat, J. Appl. Phys. **91**, 3955 (2002).
[3] K. Ennser, S. Taccheo, T. Rogowski, and J. Shmulovich, Opt. Express **14**, 10307 (2006).
[4] F. D. Patel, S. DiCarolis, P. Lum, S. Venkatesh, and J. N. Miller, IEEE Photonics Technol. Lett. **16**, 2607 (2004).
[5] K. Suk, M. Lee, J. S. Chang, H. Lee, N. Park, G. Y. Sung, and J. H. Shin, Opt. Express **18**, 7724 (2010).
[6] J. H. Shin and M. Lee, IEEE Photonics Technol. Lett. **25**, 1801 (2013).
[7] H. Isshiki and T. Kimura, IEICE Trans. Electron. **E91-C**, 138 (2008).
[8] R. M. Guo, X. J. Wang, K. Zang, B. Wang, L. Wang, L. F. Gao, and Z. P. Zhou, Appl. Phys. Lett. **99**, 161115 (2011).
[9] L. Wang, R. M. Guo, B. Wang, X. J. Wang, and Z. P. Zhou, IEEE Photonics Technol. Lett. **24**, 900 (2012).
[10] R. Kirchain and L. Kimerling, Nat. Photonics **1**, 303 (2007).
[11] R. X. Yan, D. Gargas, and P. D. Yang, Nat. Photonics **3**, 569 (2009).
[12] H. G. Park, C. J. Barrelet, Y. N. Wu, B. Z. Tian, F. Qian, and C. M. Liber, Nat. Photonics **2**, 622 (2008).
[13] P. J. Pauzauskie, D. J. Sirbuly, and P. Yang, Phys. Rev. Lett. **96**, 143903(2006).
[14] N. O. Weiss and X. Duan, Nat. Nanotechnol. **8**, 312 (2013).
[15] Y. Huang, X. Duan, and C. M. Lieber, Small **1**, 142 (2005).
[16] B. Piccione, C.-H. Cho, L. K. van Vugt, and R. Agarwal, Nat. Nanotechnol. **7**, 640 (2012).
[17] P. Berini and I. De Leon, Nat. Photonics **6**, 16 (2012).
[18] N. Liu, H. Wei, J. Li, X. R. Tian, Z. X. Wang, A. L. Pan, and H. X. Xu, Sci. Rep. **3**, 1967 (2013).
[19] S. Kéna-Cohen, P. N. Stavrinou, D. D. C. Bradley, and S. A. Maier, Nano Lett. **13**, 1323 (2013).
[20] H. J. Choi, J. H. Shin, K. Suh, H. K. Seong, H. C. Han, and J. C. Lee, Nano Lett. **5**, 2432 (2005).
[21] M. Miritello, R. Lo Savio, F. Iacona, G. Franzò, A. Irrera, A. M. Piro, C. Bongiorno, and F. Priolo, Adv. Mater. **19**, 1582 (2007).
[22] X. J. Wang, B. Wang, L. Wang, R. M. Guo, H. Isshiki, T. Kimura, and Z. Zhou, Appl. Phys. Lett. **98**, 071903 (2011).
[23] X. J. Wang, G. Yuan, H. Isshiki, T. Kimura, and Z. Zhou, J. Appl. Phys. **108**, 013506 (2010).
[24] A. L. Pan, L. J. Yin, Z. C. Liu, M. H. Sun, R. B. Liu, P. L. Nichols, Y. G. Wang, and C. Z. Ning, Opt. Mater. Express **1**, 1202 (2011).
[25] M. Fujii, M. Yoshida, Y. Kanzawa, S. Hayashi, and K. Yamamoto, Appl. Phys. Lett. **71**, 1198 (1997).
[26] M. Miritello, P. Cardile, R. Lo Savio, and F. Priolo, Opt. Express **19**, 20761 (2011).
[27] D. Martin, A. Heinzig, M. Grube, L. Geelhaar, T. Mikolajick, H. Riechert, and W. M. Weber, Phys. Rev. Lett. **107**, 216807 (2011).
[28] Y. Cui, L. J. Lauhon, M. S. Gudiksen, J. F. Wang, and M. C. Lieber, Appl. Phys. Lett. **78**, 2214 (2001).
[29] X. Fang, Z. Y. Li, Y. B. Long, H. X. Wei, R. J. Liu, J. Y. Ma, M. Kamran, H. Y. Zhao, X. F. Han, B. R. Zhao, and X. G. Qiu, Phys. Rev. Lett. **99**, 066805 (2007).
[30] Y. Akihama and K. Hane, Light Sci. Appl. **1**, e16 (2012).
[31] K. Kawano and T. Kitoh, *Introduction to Optical Waveguide Analysis: Solving Maxwell's Equations and the Schrödinger Equation* (Wiley InterScience, New York, 2001).
[32] D. Saxena, S. Mokkapati, P. Parkinson, N. Jiang, Q. Gao, H. H. Tan, and C. Jagadish, Nat. Photonics **7**, 963 (2013).
[33] See Supplemental Material at http://link.aps.org/supplemental/10.1103/PhysRevLett.115.027403, which

includes Refs. [34–41], for details of experimental methods, nanowire structure characterization, additional experiment for optical amplification, comparison with previously reported result (Table S1), and additional simulation for optical modal analysis.

[34] F. X. Gu, L. Zhang, X. F. Yin, and L. M. Tong, Nano Lett. **8**, 2757 (2008).

[35] A. Shooshtari, T. Touam, and S. I. Najafi, Opt. Quantum Electron. **30**, 249 (1998).

[36] L. M. Tong, J. Y. Lou, R. R. Gattass, S. L. He, X. W. Chen, L. Liu, and M. Eric, Nano Lett. **5**, 259 (2005).

[37] W. H. Wang, Q. Yang, F. R. Fan, H. X. Xu, and Z. L. Wang, Nano Lett. **11**, 1603 (2011).

[38] Y. C. Van, A. J. Faber, and H. de Waal, Appl. Phys. Lett. **71**, 2922 (1997).

[39] R. R. Thomson, N. D. Psaila, S. J. Beecher, and A. K. Kar, Opt. Express **18**, 13212 (2010).

[40] N. D. Psaila, R. R. Thomson, H. T. Bookey, A. K. Kar, N. Chiodo, R. Osellame, G. Cerullo, S. Shen, and A. Jha, Appl. Phys. Lett. **90**, 131102 (2007).

[41] P. Carny, J. E. Roman, F. W. Willems, M. Hempstead, J. C. vanderPlaats, C. Prel, A. Beguin, A. M. J. Koonen, J. S. Wilkinson, and C. Lerminiaux, Electron. Lett. **32**, 321 (1996).

[42] W. Shao, G. Chen, J. Damasco, X. Wang, A. Kachynski, T. Y. Ohulchanskyy, C. Yang, H. Ågren, and P. N. Prasad, Opt. Lett. **39**, 1386 (2014).

[43] N. O. Weiss and X. Duan, Proc. Natl. Acad. Sci. U.S.A. **110**, 15171 (2013).

[44] E. M. Freer, O. Grachev, X. Duan, S. Martin, and D. P. Stumbo, Nat. Nanotechnol. **5**, 525 (2010).